INDIAN JOURNAL OF SCIENCE AND TECHNOLOGY

RESEARCH ARTICLE

Removal of defects in CdO nanoparticle and rapid synthesis of CdO nanoflake using novel microwave technique to improve semiconductor device performance

Anjan Das[1]*

1 Assistant Professor, Department of Physics, Government General Degree College Singur, 712409, West Bengal, India. Tel.: +91 9434527789

OPEN ACCESS

Received: 29.12.2020

Accepted: 14.03.2021

Published: 02.04.2021

Citation: Das A (2021) Removal of defects in CdO nanoparticle and rapid synthesis of CdO nanoflake using novel microwave technique to improve semiconductor device performance. Indian Journal of Science and Technology 14(10): 858-868. https://doi.org/10.17485/IJST/v14i10.1965

* **Corresponding author**.

Tel: +91 9434527789
anjan802002@yahoo.co.in

Funding: None

Competing Interests: None

Published By Indian Society for Education and Environment (iSee)

ISSN
Print: 0974-6846
Electronic: 0974-5645

Abstract

Objective: The objective of this study is to synthesize CdO nanoparticle and nanoflakes both in a single way. Also the purpose of removing defects from semiconductor nanoparticles has been considered. **Methods**: Very small sized Cadmium oxide nanoparticles (11 – 29 nm) and nanoflakes of average size 70 nm were prepared by sol-gel process. Two solutions of 0.2M $CdCl_2$ and 0.2M NaOH were used with a mixture of 1:2 ethylene glycol and methanol. Two different heating method of dried precipitate was adopted to observe the morphology and defect characteristics. Half of the precipitate was annealed in furnace and rest half in domestic microwave. **Findings**: The fcc (NaCl-type) structure has been found in the nanostructures with lattice constant varying with annealing temperature. We propose a linear relation for the change in lattice constant. HRTEM pictures show nanoflakes and hexagonal nanoparticles. The ratio curve of coincidence Doppler broadening spectroscopy (CDBS) found defect concentration reduction and agglomeration effect on microwave irradiation in place of furnace annealing. It indicated reduction of defects inside the nanoparticles. The S and W parameter revealed the chemical surroundings and momentum distribution of the vacancy clusters varying with crystallite size. **Novelty:** Furnace annealing and microwave irradiation showed different effect of surface strain on lattice. Microwave irradiation has been used to reduce defects inside CdO nanocrystals for potential application and coincidence Doppler broadening spectroscopy showed potential to be a very effective tool of defect characterization and electron momentum comparison. Also, this work presents how microwave radiation can be used to prepare nanoflakes and nanoparticles from same reactants without any substrate.

Keywords: Domestic microwave; nanocrystals; positron annihilation; solgel processes

1 Introduction

Nowadays the nanomaterials have drawn much attention for its wide application and increase of basic knowledge in materials [1] research. The change of structural, optical and electrical properties of a metal oxide nanomaterial with its size/thickness makes it a versatile candidate in many areas of science and technology. Cadmium oxide (CdO) is a narrow band gap n type semiconductor [2,3]. Various methods have been adopted to synthesize CdO nanoparticles [4,5] to use them in technological [6] applications. Among the synthesis procedures the sol-gel process is advantageous for its low cost, [7] simple method and produces highly pure [8] size controlled nanoparticles.

Defects are often responsible for degradation in performance of a semiconductor device. Point defects can decrease the desired level of doping that can be achieved while fabricating a semiconductor device. To overcome these difficulties defect concentration should be reduced. Sometimes one wants defect concentration to be more for ultrafast optoelectronic switches or semiconductors used to optically generate THz pulses, where defect densities should be large enough so that carrier lifetimes are as short as a few picoseconds. Many researchers have reported their work on characterization [9], and electrical, optical, [10] magnetic [11] studies on CdO and other metal oxide nanomaterials. The literature available, on defect characterization and control over defect concentration and size by only changing the heating method to same precursors, is least.

In this report sol – gel method followed by annealing and microwave irradiation has been utilized to synthesize six different CdO nanosamples to obtain various crystallite sizes and nanoflakes. To the best of our knowledge nanoparticles and nanoflakes have not been prepared by same method. Nowadays annealing of dried metal hydroxide precipitates is done also by domestic microwave at 2.45 GHz at various powers [12]. Microwave irradiation method provided simple and fast routes to the synthesis of pure nanomaterials with narrow distribution of size and no high temperature or high pressure was needed. Its need to observe if any change occurs in dimensionality of nanomaterials on alteration of microwave power.

2 Experimental Details

2.1 Synthesis of samples

All reagents used were of analytical grade and provided by Merck. Two different solutions were prepared by dissolving 0.1 M $CdCl_2$ and 0.1 M NaOH in 40 ml and 200 ml distilled water respectively. Another 300 ml mixture of ethylene glycol and methanol was prepared in 1:2 ratio. Ethylene glycol mixture was added to NaOH solution and stirred for one hour. Then $CdCl_2$ solution was added and stirred for two hours. A milky white solution was obtained. Precipitate was formed by adding acetone to it. The precipitate was washed by methanol and heated to 70 °C to evaporate the methanol. Then it was kept for 24 hours for gelation and a gel in beaker was formed. It was divided in six parts. Three of the six parts were annealed in a muffle furnace of HMG India at 300 °C, 400 °C and 500 °C for 4 hours. Rest of them were treated separately in a domestic microwave manufactured by LG of model no MC2149BPB. For this purpose the microwave irradiation was carried out on those dried precipitates by keeping them in a microwave proof glass pot at 2.45 GHz for 480, 650 and 800 watt. Time duration for all of them was three minutes only.

In a domestic microwave cavity heating is generally achieved through dipolar polarization and ionic conduction. When the dipoles of irradiated molecules in solution try to align with the oscillating magnetic field, they generate heat. The amount of heat generated is related to the frequency of the field and how fast the molecules align with the field. If alignment is either very fast or very slow, little heating will occur. Inside the cavity ions also move with the oscillating field, they collide with each other and generate heat. These collisions of ions with other species in solution generate much more heat than dipolar polarization.

2.2 Characterization and coincidence Doppler broadening spectroscopy

X-ray diffraction (XRD) patterns of the samples were recorded with Bruker D8 Advance diffractometer using Cu Kα (λ = 1.5406 Å) radiation at 40 kV and 40 mA. All the samples were scanned from 20° to 85° with a scanning speed of 2° (2θ) per minute. HRTEM images were taken with a JEOL (Model JEM 2200FS) microscope operating at 200 kV. Positron annihilation spectroscopy has been carried out for defect characterization and to closely observe the core electron structure with the changes in particle size. Figure 1 shows the block diagram of CDBS set up.

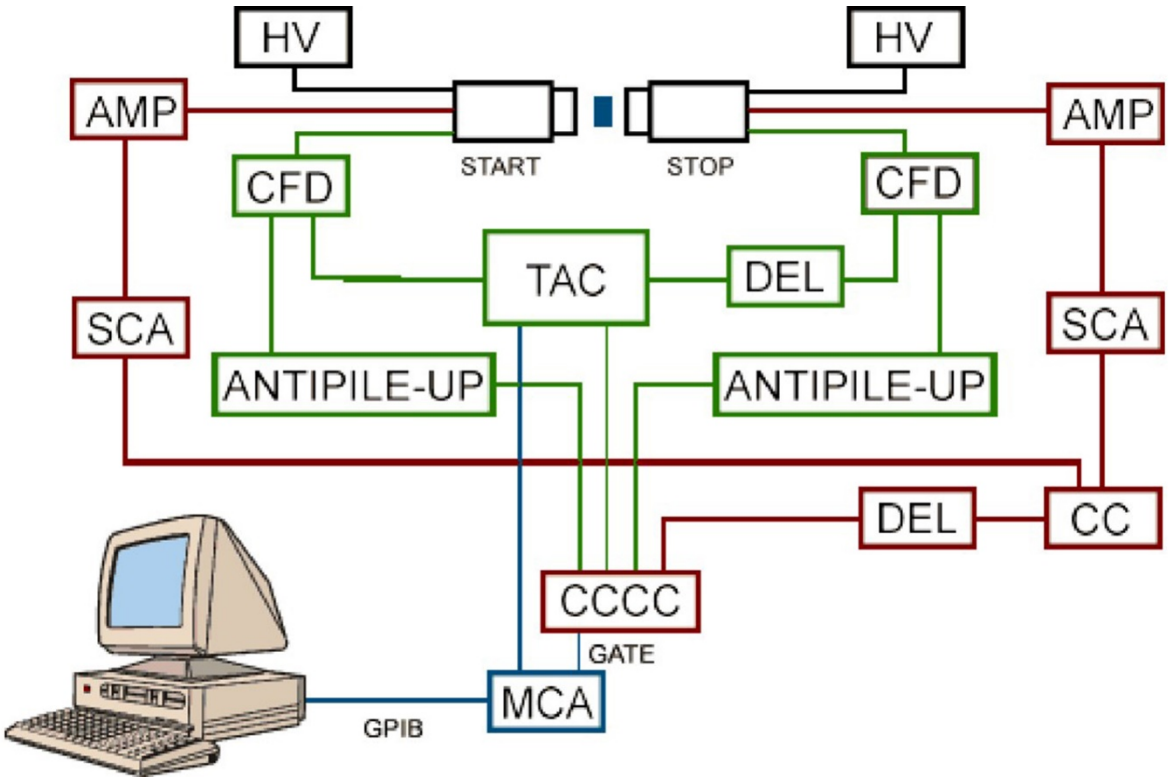

Fig 1. Block diagram of CDBS.

Block diagram of coincidence Doppler broadening spectroscopy set up. HV – High Voltage, AMP – Amplifier, SCA – Single Channel Analyzer, TAC – Time to Amplitude Converter, DEL – Direct Exchange Line, CFD – Constant Fraction Discriminator, CC – Constant Current, MCA – Multi Channel Analyzer.

To carry the coincidence Doppler broadening measurements a 10 μCi strong ^{22}Na source was used. The source was kept immersed inside a column of powdered sample taken in a glass tube. To keep the source and sample moisture free they were kept in high vacuum. Coincidence Doppler broadening (CDB) measurements were done with two high pure germanium detectors (HPGe) of energy resolution 1.33 keV and 1.27 keV at 0.511 MeV. Analysis was done with AMPS[13]. About 2.0 $\times$ 10^7 coincidence events were accumulated under CDB spectrum.

3 Results and Discussion

3.1. X – Ray diffraction spectroscopy

Figure 2 shows the XRD patterns of all CdO nanoparticulate and nanowire samples. Figure 1(a) shows the X – Ray diffraction pattern of furnace annealed samples and Figure 1(b) shows for microwave irradiated (MI) samples. Our peaks agree well with the standard values of JCPDS Card No 05-0640. The spectra show face centred cubic structure of as synthesized samples. No secondary phases were observed in the spectra of the samples except 18 nm, indicating that the synthesized samples are of high purity. The lattice constant of bulk CdO is 4.6900Å[14] whereas those of the samples synthesised in this work differed from this value on account of their nanocrystalline structure. From the most intense broadened peak width, the average crystallite sizes of the different samples were estimated by using the Debye-Scherer equation[15] and they varied from 11 nm to 24 nm. Nanocrystallite size of microwave synthesized samples are in the range 18 – 70 nm. Tables 1 and 2 show the crystallite sizes and their lattice constants. From the table, it is clear that the particle size is very sensitive to the changes in temperature or irradiation power. The lowest particle size (18 nm) of MI sample shows (Figure 2) some other peaks at 2θ = 26°, 33°, 57° and 60° positions. For less applied microwave power the amount of heat generated through dipole oscillation inside the microwave cavity will be small. The hydroxide of cadmium have not converted to oxide completely and caused some other peaks in XRD spectra with a satellite peak at around 45°.

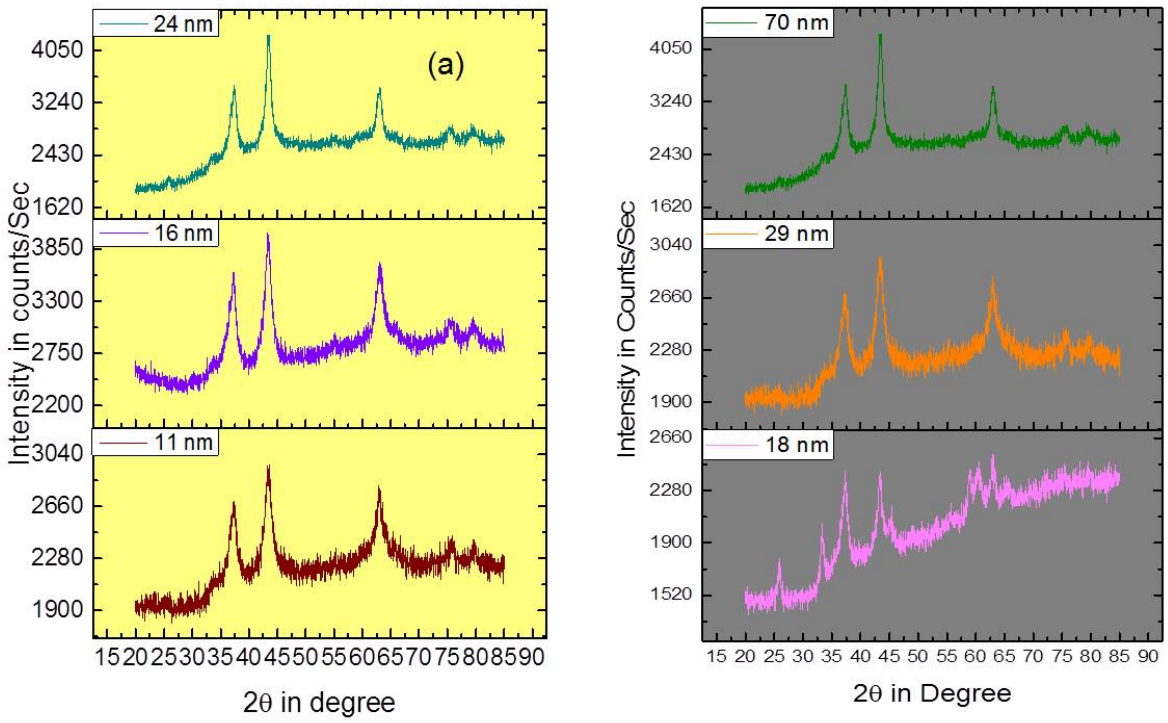

Fig 2. XRD patterns of the CdO nanocrystalline samples. (a) annealed samples, (b) MI samples

Table 1. Estimated size and lattice parameters of annealed samples

Crystallite size (nm)	Lattice parameter (Å)	Temperature (°C)	S	W
11	4.7086	300	0.47	0.68
16	4.8312	400	0.48	0.66
24	4.8952	500	0.55	0.59

Table 2. Estimated size and lattice parameters of MI samples

Crystallite size (nm)	Lattice parameter (Å)	Applied power (W)	S	W
18	4.8041	480	0.51	0.61
29	4.8047	650	0.60	0.58
70 (Nanoflake)	4.8049	800	0.61	0.56

The X – Ray diffraction peak widths were used to estimate the average crystallite sizes of samples except the nanowire by Debye – Scherrer equation

$$D = 0.9\lambda/\beta\cos\theta \tag{1}$$

where D is the average crystallite diameter, λ is the wavelength (CuKα) used by the diffractometer, β is the line width at half maximum and 2θ is the Bragg angle of scattering. It can be further observed that the peaks have gradually shifted towards lower 2θ values with increase of particle size which indicates lattice expansion. The lattice constants (a) of the different samples were estimated from the XRD data by combining the Bragg's equation with the crystallographic plane spacing (d) and getting the relation $\frac{4\sin^2\theta}{\lambda^2} = \frac{1}{d^2} = \frac{h^2+k^2+l^2}{a^2}$.

Rajesh et al[16] reported CdO synthesis by microwave irradiation where particle sizes were in the range 25 to 51 nm and nanowire was not produced. Our nanoparticles are even smaller than the CdO nanoparticles prepared by Selvam et al.[17] as they used more time of irradiation and hence surface to volume ratio in our work is greater. In this work variation of lattice constant has been observed with increased surface to volume ratio by decreasing the particle size more. Increased surface to

volume ratio leads to faster reaction rate and more frequency of collision for chemical reaction. Diehm et al.[18] have made a detailed analysis of the effect of sizes of oxide nanoparticles on the lattice parameter changes. According to their results strain mediated by structural defects like vacancies is a major cause of lattice expansion in metal oxide nanoparticles. A plot of the changes in lattice constant from its bulk value 4.6900 Å, Δa versus crystallite size is given in Figure 3.

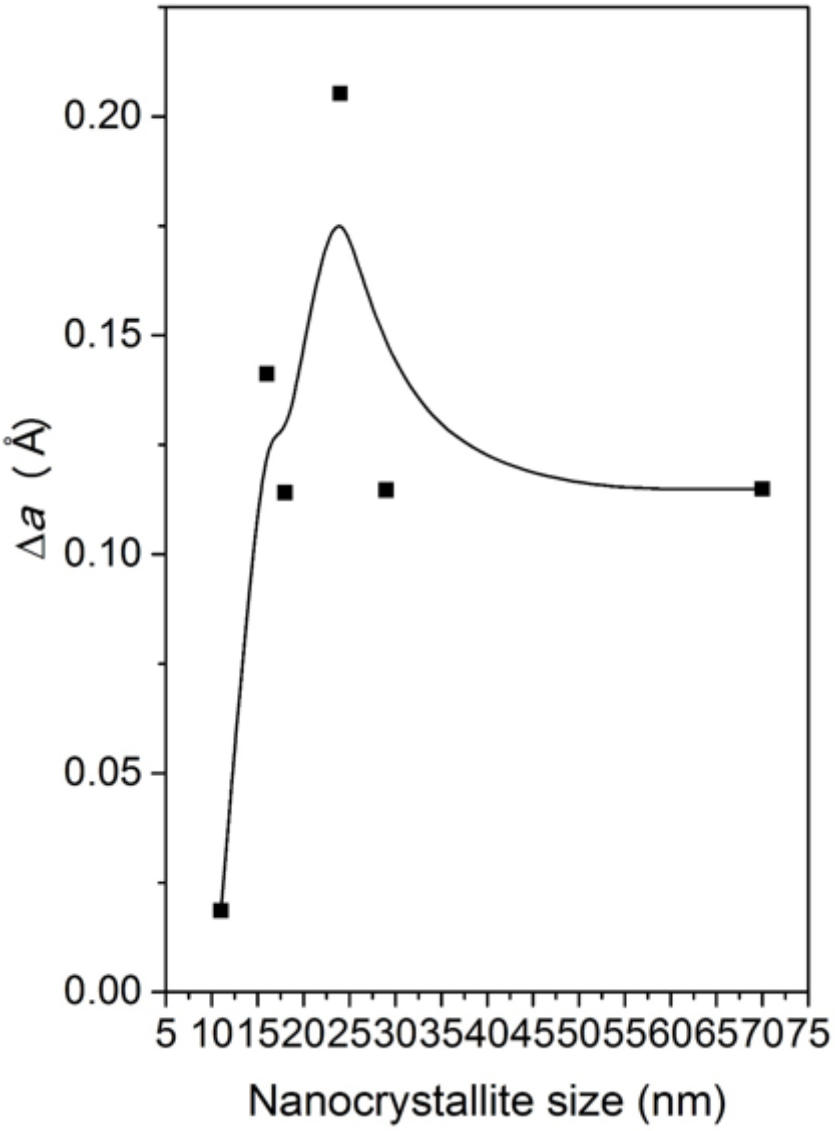

Fig 3. Changes in lattice constant Δa versus crystallite size

This behavior can be described by an equation, equation – 2, proposed for the first time here. It shows that for nanocrystallite sizes (D) in the range 11 -24 nm change in lattice constant has increased linearly as

$$\Delta a = 0.01358D - 0.1144 \quad (2)$$

with the increase in average crystallite size. According to Diehm et al. for decreasing nanocrystallite sizes, surface pressure and surface to volume ratio increases which increases the surface stress and causes lattice to contract which is observed here. This has been also found to be true after analysis of lattice strain by the Williamson – Hall method[19]. It is considered that the broadening of the X-ray diffraction peak width is due to both nanocrystallite size and lattice strain. The relation connecting the

lattice strain (ε), crystallite size (D) and full width at half maximum (β) can be written as

$$\beta cos\theta = \frac{k\lambda}{D} + 4\varepsilon sin\theta \tag{3}$$

The plot of strain versus nanocrystallite size in Figure 4 shows the relaxation of strain with increasing crystallite size. The Williamson – Hall method actually depends on many parameters and it has been approximated that strain is uniform in all directions of crystallographic planes. The decreasing strain changes its trend remarkably after 24 nm and increases to saturate. The decrease of lattice constant with decreasing particle size, can result from strain induced by the increasing number of surface atoms (i.e. the atoms less surrounded by neighbor atoms) in an effort to minimize the surface free energy. Unlike in a bulk solid or coarse crystallite where the number of core atoms far outnumber the surface atoms and offer stiff resistance to surface reduction, the inner core of a nanoparticle is soft enough to contract in order to facilitate the minimization of surface energy.

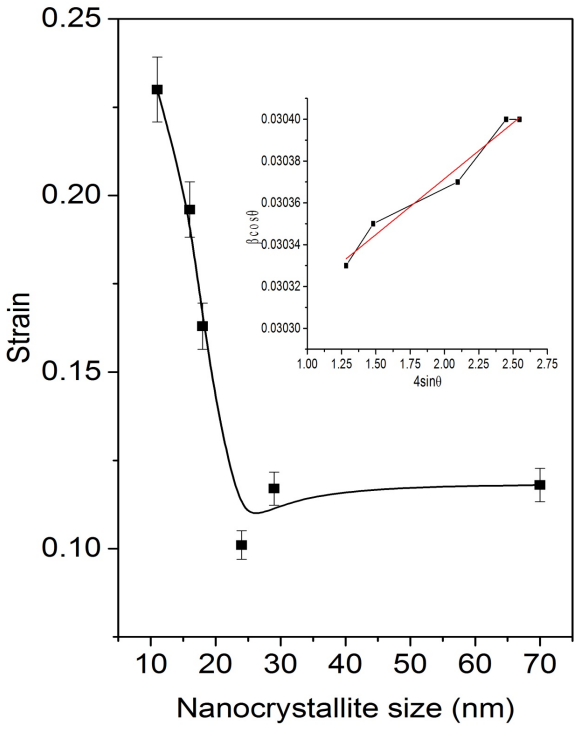

Fig 4. Strain versus nanocrystallite size. Inset contains Williamson- Hall plot.

3.2 HRTEM analysis

Figure 5 shows HRTEM images of the samples. The figure consists of CdO nanoflakes of diameter 70 nm, SAED pattern of nanoparticles, hexagonal nanoparticles and clearly visible lattice fringes. Figure 4(c) shows particles are hexagonal and uniformly distributed around 16 nm in size. Peng et al reported [20] similar kind of CdO nanomaterial synthesized by electrochemical deposition with vapour – liquid – solid mechanism but no nanoparticles were produced. The nanoflakes produced by 800 W microwave irradiation in three minute are of smaller length with same diameter. From the HRTEM data it can be seen that these nanoflakes [21] are dispersed in nature. As far as the particle sizes are concerned, the HRTEM data confirms the XRD results and shows that the nanoparticles are evenly distributed. Also, they contain lesser number of defects than annealed nanoparticles which will be evident from Coincidence Doppler broadening spectroscopy discussed later.

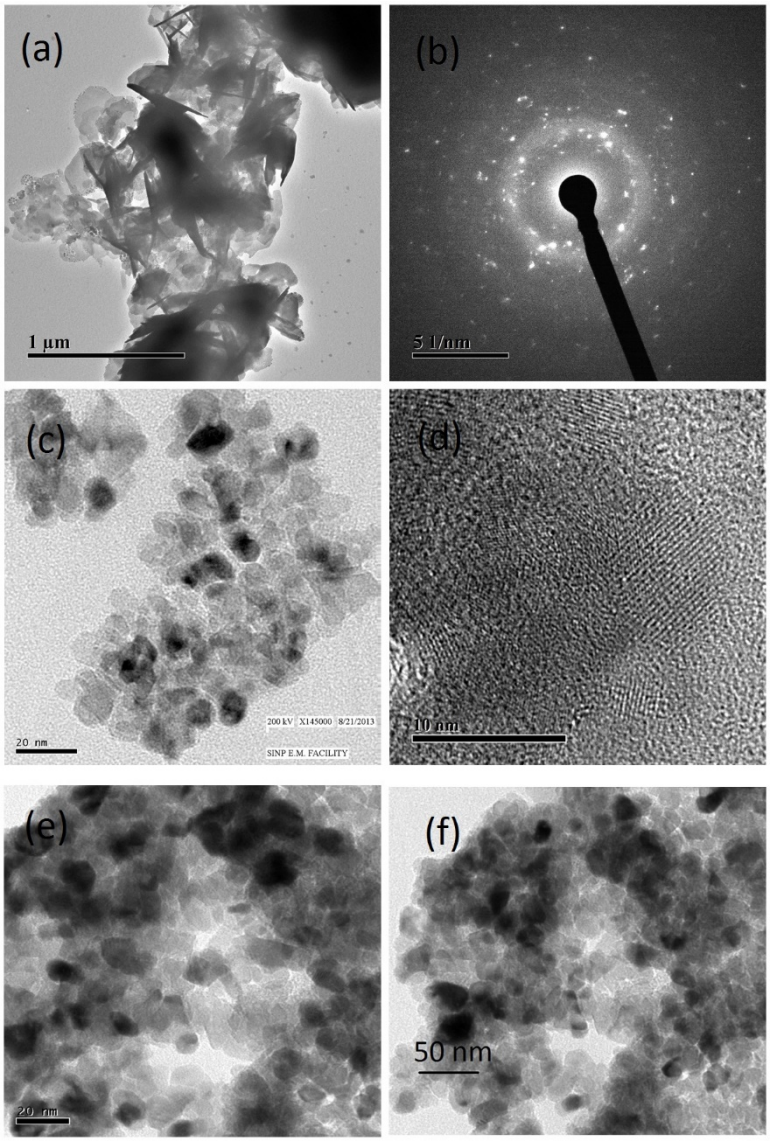

Fig 5. HRTEM images of (a) 70 nm nanowire, (b) SAED pattern of 24 nm samples, (c) 16 nm sample (d) lattice fringes of 29 nm sample (e) 11 nm sample and (f) 18 nm sample

3.3 Coincidence doppler broadening analysis

Preparation of semiconductor nanoparticles through two different heating process can cause defect characteristics to differ. The relative variation of positron – electron annihilation parameters of the different elements present in a sample can be understood with Coincidence Doppler broadening measurements. The momentum conservation during the annihilation process gives a tool to study the momentum distribution of electrons in the interior of defects in a solid. An advantage of the momentum distribution techniques is their sensitivity to the chemical environment of the annihilation site, which is higher compared with positron lifetime spectroscopy. This is because the momentum distribution information is more influenced by the chemical surroundings than the electron density[22]. The results of CDBS measurements are illustrated in Figure 5. The momentum of the positron after coming to thermal equilibrium inside a semiconductor becomes significantly smaller than electrons. After annihilation with electrons the energy released becomes Doppler shifted. The figure shows the ratio curves obtained from the one-dimensional projection of Doppler shifted energy distribution along the energy absorption channel and dividing the same by an identical distribution of Cadmium

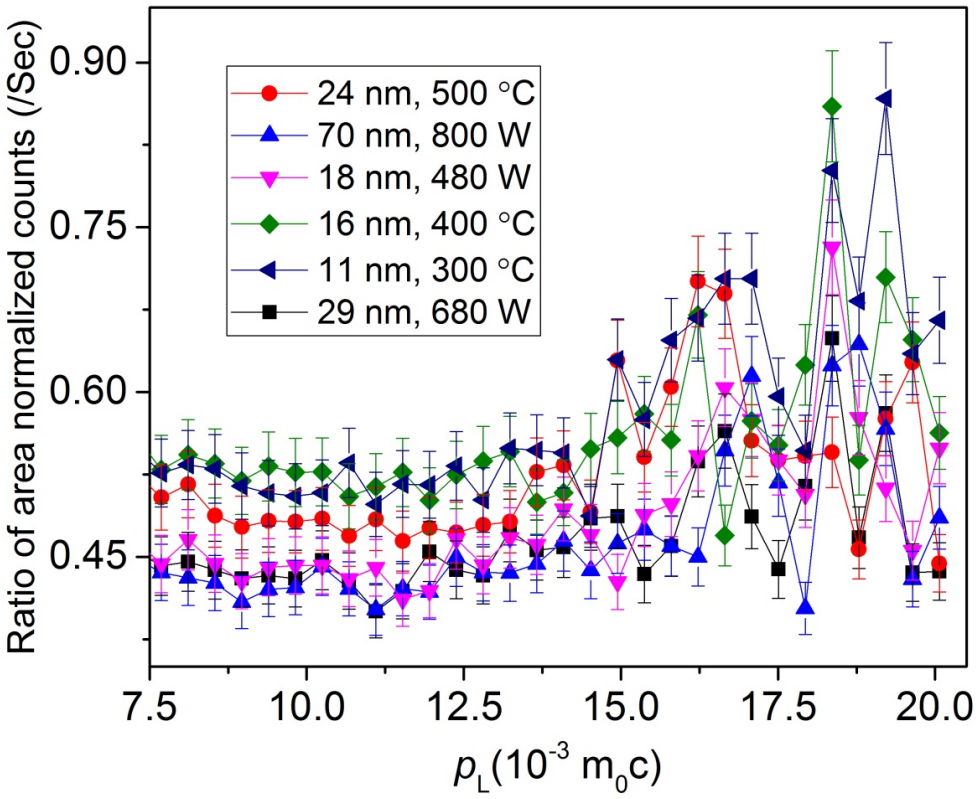

Fig 6. (color online) CDBS ratio curves of samples with respect to that of an identical curve for pure and annealed Cd foil

foil as a reference sample. The presence of cationic monovacancy inside a defect due to absence of a Cd^{2+} ion denoted as V_{Cd} becomes negatively charged and hence can attract positrons to it. A characteristic peak is observed on wings region at $p_L = 18.3 \times 10^{-3}\ m_0c$ in the spectra of the samples. The 11 nm sample exhibited its peak at $19.2 \times 10^{-3}\ m_0c$. These peaks are attributed to positron annihilation with the 2p electrons of O^{2-} ions [23] and it indicates the trapping and annihilation of positrons in the cationic vacancies [24] or vacancy clusters. Positron annihilation in nanocrystallite surfaces is ruled out for higher crystallite sizes as thermal diffusion length for metal oxides remain in the range 14 nm to 25 nm [25]. Defects inside a nanocrystallite undergo changes in size, concentration and chemical surroundings on variation of synthesis parameters, is to be considered here. Though the annihilation energy has been Doppler shifted for all nanocrystalline samples, the ratio of normalized counts presented the most promising feature of microwave irradiation to metal oxide semiconductor nanoparticles. It has been found from Figure 5 that the ratio of normalized counts are higher for annealed samples than MI samples keeping the peaks almost in same position except 11 nm sample. This difference indicates marked difference in number of high momentum electron – positron annihilation for differently synthesized samples. Here it can be inferred that for annealed samples the defect concentration is greater than MI samples. In sol – gel process when heat is supplied to the dried gel inside an electric furnace, agglomeration of particles and formation of network throughout the gel are dependent on the time as well as mechanism also. On the other hand inside a microwave cavity when the dried precipitate or gel is irradiated, dipole oscillation of molecules of precipitate and movement of ions set in depending on frequency and power. The amount of heat generated depends on frequency of the microwave radiation and applied power. How fast the dipoles align [26] depends on applied power. If alignment is either very fast or very slow, little heating will occur. Kumari et al. [27] prepared undoped and doped CdO nanomaterials in a fixed temperature and studied electrical properties. They studied resistivity of the samples prepared. In this work increasing microwave power increased the nanocrystallite size. In the synthesis of 18 nm sample the alignment of dipoles of the precipitate is slow whereas in case of 46 nm sample the alignment is very fast. In both cases the heat generation is low. The variations of normalized counts

with electron momentum can provide us information about defect agglomeration with alteration of synthesis procedure, rate of increase of heat and time given for heat supply to dried gel. For annealed samples the higher values of counts in CDBS spectra follows from the fact that numerous defects did not undergo agglomeration effect. Size of the vacancy type defects and width of grain boundaries remained less or increased in very small amount. On the other hand the comparatively less ratio normalized counts of MI samples shows us the efficiency of microwave synthesis procedure towards reducing the number of defects per volume i.e. concentration by agglomerating the defects and sometimes it can nearly anneal out the defects. Though from the work of Rajput et al. [28] we come to know that CdO nanoflakes have good conductivity, it is mentionable that concentration and size of defects play important role in majority carrier conduction inside semiconductors for which S and W parameter study is helpful.

The S and W parameters revealed the scenario of high and low momentum electrons inside defects. The S-parameter is calculated from its definition – the ratio of the counts under central area of the 511 keV photo peak to the total counts under the whole spectrum. The S-parameter represents the fraction of positrons annihilating with the electrons of low momentum with respect to the total number of annihilated electrons. The W-parameter is the ratio of the counts in the wings of the curve of detected gamma radiation to the total, representing high momentum core electrons. From the plot of S parameter vs crystallite size (Figure 6) it can be seen that S increases (Figure 4 a) when crystallite size increases and reaches a saturation level from 29 nm.

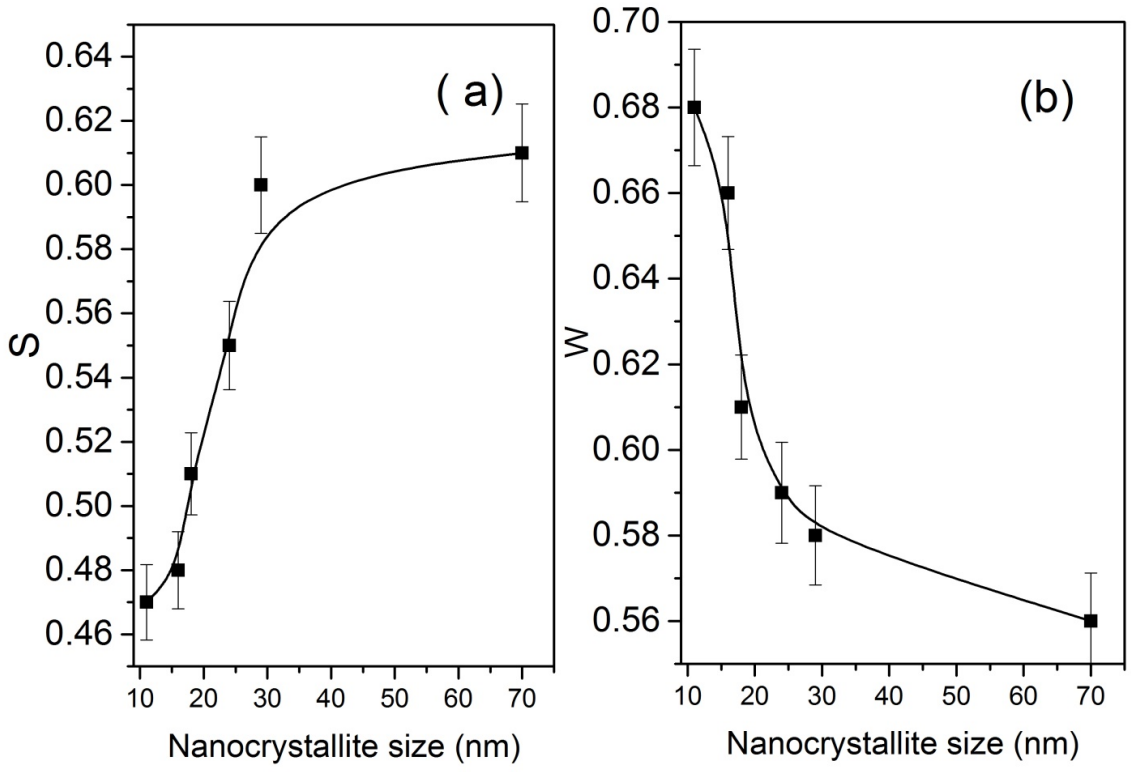

Fig 7. Variation of S and W parameter of samples with nanocrystallite size

The initial slow increase of S indicates start of vacancy clustering inside the nanoparticles. The defect agglomeration reaches its highest level on largest size i.e. nanowire for microwave irradiated samples. The CDBS ratio curve shows the peak of 11 nm sample again shifting towards higher momentum side. This sample exhibited some XRD peaks related to $Cd(OH)_2$. The shift towards higher momentum area supports our earlier observation that all part of the gel did not convert to CdO nanoparticle and remained as hydroxide. When nanocrystallite size increases the surface to volume ratio decreases as more and more molecules are gathered inside a particle and increases the volume. The variation of S may have been influenced by the formation of

positronium states also inside the larger nanoparticles. The increase of annealing temperature and irradiation power forces the vacancy-type defects to agglomerate. The W parameter has shown an increasing trend with decrease of crystallite size. From the variations of S and W parameters it can be said that the defect clusters that trap positrons basically remain of the same origin and configuration. In other words, the surface contribution to the annihilation characteristics of the positrons is negligible and other potential positron trapping defects such as dislocations and loops are practically absent in the samples.

Investigation on CdO nanomaterial is in fast root. These are summarized in Table 3. Variation of lattice constant, particle size, strain and adopted annealing procedure can be compared with each other. From Figure 3 and Table 2 it has been found that the increasing microwave irradiation, which might be a novel approach on reducing the strain that in turn keeps the lattice constant almost same. Various morphologies of CdO nanostructure has been prepared as summarized in Table 4 but defect characterization by CDBS is a have to be added. Metal oxide nanoparticles can be synthesized in many ways, but they need special attention to remove or reduce the defects inside them such that they can be applied in semiconductor technology efficiently. Thanks to continuous development of microwave reactors for synthesis of nanomaterials[29]. In present work the semiconducting properties of CdO nanoparticles and nanoflakes have been improved not only by reducing the defects but also reducing the particle size and prepared nanoflakes for possible technological applications. Generally adopting one synthesis procedure cannot show us the change in defect concentration and size. Annealing inside a furnace and inside a micro oven presented different scenario of defect characteristics.

Table 3. Comparison of XRD study

Temperature range (°C)/ Applied power	Change in lattice parameter (Å)	Particle size (nm)	Annealing procedure	Strain analysis	Ref
450 °C	+ 0.004	28 – 45	furnace	Not done	[28]
800 W	+ 0.0053	78	MI	Not done	[17]
500 °C	- 0.002 to 0.010	17.99 to 21.15	furnace	Not done	[30]

Table 4. Electrical properties of CdO nanomaterials

Ref	Morphology	Conductivity study	Morphology type	CDBS
[28]	Nanoflower in substrate	Good conductivity	One	Not done
[30]	Heterojunction	Charge carrier	One	Not done
[17]	Nanoparticle	None	One	Not done

4 Conclusion

Cadmium oxide nanoparticles by sol – gel process has been successfully synthesized in two different ways of crystal growth. Highest applied power of microwave irradiation efficiently produced CdO nanoflakes from same precursors for the first time. The two different heating processes revealed many differences of structural, morphological and electrical properties of synthesized nanoparticles and nanoflakes with respect to other single synthesis methods. Use of lesser time produced smaller nanoparticles than previously reported CdO nanoparticles with higher purity. A mathematical relation has been proposed relating change in lattice constant from its bulk value with nanocrystallite size. It has been found that low temperature of furnace or low power of microwave can not convert hydroxide into oxide completely. Surface strain analysis by Williamson – Hall method proved that strain decreases with temperature and causes lattice to expand but microwave irradiation power does not change the lattice constant which has been found in earlier works shown in Table 3. Microwave synthesis method produced nanoparticles with lesser number of defects for first time. Microwave irradiation is very efficient to reduce the defect concentration which in turn kept lattice constant almost same even after increase in size of nanocrystals. The estimated S and W parameters also showed that the momentum of electrons decorating the defect walls are influenced by synthesis procedure. The CDBS spectra are indicative of hydroxide remains from precursors and size and concentration variations of defects due to two synthesis roots. Based on our work we propose new opportunities for nanoparticle synthesis offered by microwave heating and it can be safely said that CDBS is a very good probe of atomic level for material characterization.

Acknowledgement

The author is grateful on Dr. Goutam Das of National Metallurgical Laboratory, Jamshedpur, India for his help and advice on XRD and HRTEM.

References

1) Das A, Mandal AC, Roy S, Nambissan PMG. Internal defect structure of calcium doped magnesium oxide nanoparticles studied by positron annihilation spectroscopy. *AIP Advances*. 2018;8(9). Available from: https://dx.doi.org/10.1063/1.5001105.
2) Radi PA, Brito-Madurro AG, Madurro JM, Dantas NO. Characterization and properties of CdO nanocrystals incorporated in polyacrylamide. *Brazilian Journal of Physics*. 2006;36(2a):412–414. Available from: https://dx.doi.org/10.1590/s0103-97332006000300048.
3) Somasundaram G, Rajan J, Sangaiya P, Dilip R. Hydrothermal synthesis of CdO nanoparticles for photocatalytic and antimicrobial activities. *Results in Materials*. 2019;4. Available from: https://dx.doi.org/10.1016/j.rinma.2019.100044.
4) Vadgama VS, Vyas RP, Jogia BV, Joshi MJ. Synthesis and characterization of CdO nano particles by the sol-gel method. In: and others, editor. Aip Conference Proceedings;vol. 1873. 2017. Available from: https://doi.org/10.1063/1.4982100.
5) Vinogradov AV, Vinogradov VV. Low-temperature sol–gel synthesis of crystalline materials. *RSC Adv*. 2014;4(86):45903–45919. Available from: https://dx.doi.org/10.1039/c4ra04454a.
6) Kumar A, Kuang Y, Liang Z, Sun X. Microwave chemistry, recent advancements, and eco-friendly microwave-assisted synthesis of nanoarchitectures and their applications: a review. *Materials Today Nano*. 2020;11. Available from: https://dx.doi.org/10.1016/j.mtnano.2020.100076.
7) Cano-Casanova L, Amorós-Pérez A, Lillo-Ródenas M, Román-Martínez M. Effect of the Preparation Method (Sol-Gel or Hydrothermal) and Conditions on the TiO2 Properties and Activity for Propene Oxidation. *Materials*. 2018;11(11). Available from: https://dx.doi.org/10.3390/ma11112227.
8) Lazareva SV, Shikina NV, Tatarova LE, Ismagilov ZR. Synthesis of High-Purity Silica Nanoparticles by Sol-Gel Method. *Eurasian Chemico-Technological Journal*. 2017;19(4). Available from: https://dx.doi.org/10.18321/ectj677.
9) Zahera M, Khan SA, Khan IA, Sharma RK, Sinha N, Al-Shwaiman HA, et al. Cadmium oxide nanoparticles: An attractive candidate for novel therapeutic approaches. *Colloids and Surfaces A: Physicochemical and Engineering Aspects*. 2020;585:124017–124017. Available from: https://dx.doi.org/10.1016/j.colsurfa.2019.124017.
10) Zafer S. Synthesis and optical properties of uranium-doped cadmium oxide synthesized by sol-gel method. *Materials Science-Poland*. 2020;38:23–27. Available from: https://doi.org/10.2478/msp-2020-0017.
11) Tawfik WZ, Esmat M, El-Dek SI. Drastic improvement in magnetization of CdO nanoparticles by Fe doping. *Applied Nanoscience*. 2017;7(8):863–870. Available from: https://dx.doi.org/10.1007/s13204-017-0623-6.
12) Rashidzadeh M, Carbajal-Franco G, Tiburcio-Silver A. Hydrophobic Coatings Composed by Cubic-Shaped CdO Nanoparticles Grown by a Novel and Simple Microwave Method. *Journal of Nanoparticles*. 2016;2016:1–6. Available from: https://dx.doi.org/10.1155/2016/8389647.
13) 13.Linux Advanced MultiParameter System. . Available from: http://www.tifr.res.in/~pell/lamps.html.
14) Mariammal RN, Susila VM, Ramachandran K. On the Debye-Waller factor and Debye temperature of CdO nanoparticles. *Crystal Research and Technology*. 2011;46(9). Available from: https://dx.doi.org/10.1002/crat.201100138.
15) Cullity B. Elements of X-ray Diffraction. Reading, Massachusetts. Addison-Wesley Publishing Company: Inc. 1956.
16) Rajesh N, Kannan JC, Krishnakumar T, Neri G. Microwave Irradiation Effect on Structural, Optical, and Thermal Properties of Cadmium Oxide Nanostructure. *Acta Physica Polonica A*. 2014;125(5):1229–1235. Available from: https://dx.doi.org/10.12693/aphyspola.125.1229.
17) Selvam NCS, Kumar RT, Yogeenth K, Kennedy LJ, Sekaran G, Vijaya JJ. Simple and rapid synthesis of Cadmium Oxide (CdO) nanospheres by a microwave-assisted combustion method. *Powder Technology*. 2011;211(2-3):250–255. Available from: https://dx.doi.org/10.1016/j.powtec.2011.04.031.
18) Diehm PM, Ágoston P, Albe K. Size-Dependent Lattice Expansion in Nanoparticles: Reality or Anomaly? *ChemPhysChem*. 2012;13(10):2443–2454. Available from: https://dx.doi.org/10.1002/cphc.201200257.
19) Williamson GK, Hall WH. X-ray line broadening from filed aluminium and wolfram. *Acta Metallurgica*. 1953;1(1):22–31. Available from: https://dx.doi.org/10.1016/0001-6160(53)90006-6.
20) Peng XS, Wang XF, Wang YW, Wang CZ, Meng GW, Zhang LD. Novel method synthesis of CdO nanowires. *Journal of Physics D: Applied Physics*. 2002;35(20):L101–L104. Available from: https://dx.doi.org/10.1088/0022-3727/35/20/103.
21) Wang Q, Chen Y, Aiyiti A, Zheng M, Li N, Xu X. Scaling behavior of thermal conductivity in single-crystalline α-Fe2O3 nanowires. *Chinese Physics B*. 2020;29(8). Available from: https://dx.doi.org/10.1088/1674-1056/ab90f0.
22) Das A, Mandal AC, Roy S, Nambissan PMG. Mn-Doping in NiO Nanoparticles: Defects-Modifications and Associated Effects Investigated Through Positron Annihilation Spectroscopy. *Journal of Nanoscience and Nanotechnology*. 2016;16(4):4153–4163. Available from: https://dx.doi.org/10.1166/jnn.2016.10963.
23) Das A, Mandal AC, Nambissan PMG. Effect of size on momentum distribution of electrons around vacancies in NiO nanoparticles. *Chinese Physics B*. 2015;24(4). Available from: https://dx.doi.org/10.1088/1674-1056/24/4/046102.
24) Ghasemifard M, Ghamari M, Samarin S, Williams JF. Porosity evaluation and positron annihilation study of mesoporous aluminum oxy-hydroxide ceramics. *Applied Physics A*. 2020;126(6):477–488. Available from: https://dx.doi.org/10.1007/s00339-020-03657-5.
25) Nieminen RM, Manninen MJ. Positrons in Solids Springer Series. In: Hautojarvi P, et al., editors. Topics in Current Physics;vol. 12. Springer. 1979;p. 145–195.
26) Wojnarowicz J, Chudoba T, Lojkowski W. A Review of Microwave Synthesis of Zinc Oxide Nanomaterials: Reactants, Process Parameters and Morphologies. *Nanomaterials*. 2020;10(6). Available from: https://dx.doi.org/10.3390/nano10061086.
27) Kumari R, Kumar V. Impact of zinc doping on structural, optical, and electrical properties of CdO films prepared by sol-gel screen printing mechanism. *Journal of Sol-Gel Science and Technology*. 2020;94:648–657. Available from: https://doi.org/10.1007/s10971-019-05202-0.
28) Rajput JK, Pathak TK, Swart HC, Purohit LP. Synthesis of CdO Nanoflowers by Sol-Gel Method on Different Substrates with Photodetection Application. *physica status solidi (a)*. 2019;216(20). Available from: https://dx.doi.org/10.1002/pssa.201900093.
29) Dąbrowska S, Chudoba T, Wojnarowicz J, Łojkowski W. Current Trends in the Development of Microwave Reactors for the Synthesis of Nanomaterials in Laboratories and Industries: A Review. *Crystals*. 2018;8(10). Available from: https://dx.doi.org/10.3390/cryst8100379.
30) Mano G, Harinee S, Sridhar S, Ashok M, Viswanathan A. Microwave assisted synthesis of ZnO-PbS heterojuction for degradation of organic pollutants under visible light. *Scientific Reports*. 2020;10(1):2224–2238. Available from: https://dx.doi.org/10.1038/s41598-020-59066-4.